

Transient aging in fractional Brownian and Langevin-equation motion

Jochen Kursawe,¹ Johannes Schulz,² and Ralf Metzler^{1,3,4}

¹*Wolfson Centre for Mathematical Biology, Mathematical Institute, University of Oxford, Oxford OX2 6GG*

²*Physics Department, Technical University of Munich, 85747 Garching, Germany*

³*Institute of Physics & Astronomy, University of Potsdam, 14776 Potsdam-Golm, Germany*

⁴*Department of Physics, Tampere University of Technology, FI-33101 Tampere, Finland*

(Received 23 July 2013; published 12 December 2013)

Stochastic processes driven by stationary fractional Gaussian noise, that is, fractional Brownian motion and fractional Langevin-equation motion, are usually considered to be ergodic in the sense that, after an algebraic relaxation, time and ensemble averages of physical observables coincide. Recently it was demonstrated that fractional Brownian motion and fractional Langevin-equation motion under external confinement are transiently nonergodic—time and ensemble averages behave differently—from the moment when the particle starts to sense the confinement. Here we show that these processes also exhibit transient aging, that is, physical observables such as the time-averaged mean-squared displacement depend on the time lag between the initiation of the system at time $t = 0$ and the start of the measurement at the aging time t_a . In particular, it turns out that for fractional Langevin-equation motion the aging dependence on t_a is different between the cases of free and confined motion. We obtain explicit analytical expressions for the aged moments of the particle position as well as the time-averaged mean-squared displacement and present a numerical analysis of this transient aging phenomenon.

DOI: [10.1103/PhysRevE.88.062124](https://doi.org/10.1103/PhysRevE.88.062124)

PACS number(s): 05.70.Ln, 02.50.-r, 05.40.-a, 87.15.Vv

I. INTRODUCTION

Normal Brownian diffusion processes are stationary in the sense that physical quantities such as two-point correlation functions $C(t_1, t_2)$ only depend on the difference of the two times t_1 and t_2 , $C(t_1, t_2) = C(|t_1 - t_2|)$. Moreover, they are independent of the time difference t_a between initiation of the process at $t = 0$ and start of the measurement at the aging time t_a . For anomalous diffusion processes, characterized by a mean-squared displacement (MSD) of the form $\langle x^2(t) \rangle \simeq K_\alpha t^\alpha$ with the generalized diffusion coefficient K_α of physical dimension $\text{cm}^2/\text{sec}^\alpha$, stationarity is not necessarily fulfilled. In both the subdiffusive ($0 < \alpha < 1$) and superdiffusive ($\alpha > 1$) regimes, physical observables may be nonergodic and exhibit an explicit dependence on the aging time t_a .

Such consequences of nonstationary behavior may be illustrated by means of the time-averaged MSD

$$\overline{\delta^2(\Delta)} = \frac{1}{T - \Delta} \int_{t_a}^{t_a + T - \Delta} [x(t + \Delta) - x(t)]^2 dt. \quad (1)$$

It evaluates a measured single-particle trajectory in terms of the sliding average along the time series $x(t)$ of length T (the process time) over the squared position differences as separated by the lag time Δ . This definition of the time-averaged MSD is typically used to analyze trajectories recorded in experiments or simulations [1,2]. Here we denote time averages by an overline. For trajectories of finite length, the additional average over sufficiently many trajectories with label i , $\langle \overline{\delta^2(\Delta)} \rangle = (1/N) \sum_{i=1}^N \overline{\delta^2(\Delta)}_i$, provides a smooth functional behavior. The quantity $\overline{\delta^2(\Delta)}$ contrasts the more standard ensemble MSD $\langle x^2(t) \rangle = \int x^2 P(x, t) dx$, defined as the spatial average of x^2 over the probability density function $P(x, t)$, which denotes the probability of the tracer particle to be at position x at time t .

The integrand in expression (1) for the time-averaged MSD $\overline{\delta^2(\Delta)}$ of a random-walk process may be expressed as the

product of the typical squared length per jump $\langle \delta x^2 \rangle$ and the average number of jumps $\langle n(t + \Delta, t) \rangle$ performed in the time interval between t and $t + \Delta$ [3,4]. For Brownian motion, the number of jumps is given by the length of the interval Δ divided by the typical time τ per jump, that is, $\langle n(t + \Delta, t) \rangle = \Delta/\tau$. Defining the diffusion constant as $K_1 = \langle \delta x^2 \rangle/[2\tau]$, after integration over t we find that $\overline{\delta x^2(\Delta)} = 2K_1 \Delta$ for any finite T [5]. This result is independent of the aging time t_a and the length T of the time series: We say that the process does not age. Moreover, it is ergodic in the sense that $\langle \delta^2(\Delta) \rangle = \overline{\delta^2(\Delta)}$. For sufficiently large T the process is self-averaging in the sense that on average each jump occurs after the time increment τ and thus a single trajectory $x(t)$ produces the result $\overline{\delta x^2(\Delta)} = 2K_1 \Delta$ such that the time-averaged MSD of different trajectories is fully reproducible [4,5].

In contrast, processes described by the Scher-Montroll continuous-time random-walk (CTRW) model with a power-law distribution $\psi(\tau) \simeq \tau^{-1-\alpha}$ ($0 < \alpha < 1$) of waiting times τ between successive jumps [6] exhibit a so-called weak ergodicity breaking [7] $\langle \delta^2(\Delta) \rangle \neq \overline{\delta^2(\Delta)}$: While the ensemble-averaged MSD scales sublinearly with time $\langle x^2(t) \rangle \simeq K_\alpha t^\alpha$, the time-averaged MSD is linear in the lag time $\overline{\delta^2(\Delta)} \simeq K_\alpha \Delta/T^{1-\alpha}$ but depends on the measurement time T [4,8]. Under confinement, $\langle x^2(t) \rangle$ reaches the thermal plateau value $\langle x^2 \rangle_{\text{th}}$ [9], while $\overline{\delta^2(\Delta)} \simeq (\Delta/T)^{1-\alpha}$ continues to grow in power-law fashion [10,11]. Such weakly nonergodic dynamics in the absence and presence of confinement was indeed observed experimentally in both the walls and the bulk volume of living biological cells [12–14]. Interestingly, a similar weak ergodicity breaking is obtained for time- and space-correlated CTRWs [15] and superaging systems [16] as well as for Markovian diffusion with scaling forms of the position dependence of the diffusion coefficient [17]. In superdiffusive systems the ergodic violation becomes ultraweak in the sense that $\langle x^2(\Delta) \rangle$ and $\overline{\delta^2(\Delta)}$ differ only by a constant factor [18]. Moreover, the aging dependence on t_a was derived for a

subdiffusive CTRW, in which the aging time t_a explicitly enters the expressions for both $\langle x^2(t) \rangle$ and $\delta^2(\Delta)$ [3,19]. For the time-averaged MSD the aging time t_a enters solely through a multiplicative factor, independent of the process details [3].

Here we are interested in the aging properties of another popular class of anomalous diffusion models: Fractional Brownian motion (FBM) and fractional Langevin-equation (FLE) motion are driven by stationary Gaussian but power-law-correlated nonwhite noise and algebraically reach ergodic behavior $\delta^2(\Delta) \sim \langle x^2(\Delta) \rangle$ in the case of free, unconfined motion [20] and $\delta^2(\Delta) \sim 2\langle x^2 \rangle_{\text{th}}$ for confined motion [21–23]. Fractional Brownian motion and FLE motion in the overdamped regime behave similarly and both emanate as effective one-particle descriptions in many-particle systems such as viscoelastic environments, single-file diffusion, or the motion of a monomer in a long polymer chain [24–27]. The ergodic nature of FBM and FLE anomalous diffusion was observed for the motion of telomeres in cell nuclei [28], the diffusion of tracers in the cytoplasm of biological cells at sufficiently long times [12,26,29], or for the motion of simulated lipid molecules in bilayers in different physical phases [30]. However, in contrast to the exponential relaxation $\langle x^2(t) \rangle \sim \langle x^2 \rangle_{\text{th}}(1 - \text{const}t^{\alpha-2} \exp\{-\text{const}t\})$ of the ensemble-averaged MSD under confinement, the time-averaged MSD of FBM exhibits the power-law approach $\delta^2(\Delta) \sim 2\langle x^2 \rangle_{\text{th}}(1 - \text{const}\Delta^{\alpha-2})$ [22]. We call this a transiently nonergodic behavior. Such a power-law relaxation of the time-averaged MSD was recently observed experimentally for microbeads tracked by optical tweezers in a wormlike micellar solution [31].

Similar to the observation of weakly nonergodic behavior in FBM or FLE motion also the transient aging behavior of these processes may become relevant under certain experimental conditions such that the influence of the aging time t_a remains detectable during the measurement. Given the temporal resolution of modern spectroscopic or single-particle tracking methods, this may be possible. Even more so, this question may become relevant in simulation studies in which extremely high time resolution is possible. Here we derive the different patterns of transient aging in the FBM-FLE family of processes fueled by power-law-correlated Gaussian noise. Thus we find that the time-averaged MSD splits into two additive terms: a stationary term depending solely on the lag time Δ and an aging term that decays with both aging time t_a and process time T . For both FBM and FLE motion the dependence on the process time T is inversely proportional. For confined FBM we obtain an exponentially fast decay in t_a , while for FLE motion we find an algebraic decay in the aging time. Interestingly, the scaling exponent is different between free and confined FLE motion.

The paper is structured as follows. After a definition of fractional Gaussian noise and an introduction to the FLE and FBM in terms of their dynamic equations in Sec. II, in Secs. III–V we discuss the ensemble- and time-averaged moments as well as the ergodic and aging behavior of free and confined FLE motion and confined FBM. In Sec. VI we draw our conclusions. In the Appendixes we describe the simulation procedure to create stochastic trajectories $x(t)$ and collect results for the autocorrelation functions.

II. ANOMALOUS DIFFUSION MODELS WITH POWER-LAW-CORRELATED GAUSSIAN NOISE

We investigate two variants of stochastic differential equations, both driven by so-called fractional Gaussian noise. These comprise the FLE, in which the fluctuation-dissipation relation [32] is satisfied, and FBM, in which the noise is external and the motion therefore is not thermalized. The associated simulation schemes are compiled in Appendix A.

Fractional Gaussian noise, the derivative process of FBM [33,34], has zero mean $\langle \xi_H(t) \rangle = 0$ and the variance ($0 < H < 1$)

$$\langle \xi_H(t_1)\xi_H(t_2) \rangle = 2D_H H(2H-1)|t_1-t_2|^{2H-2} + 4D_H H|t_2-t_1|^{2H-1}\delta(t_2-t_1), \quad (2)$$

exhibiting a power-law decay with scaling exponent $2H-2$ of the difference between the two times t_1 and t_2 . Here H denotes the Hurst exponent. Integration of fractional Gaussian noise over time results in FBM with the anomalous diffusion exponent $\alpha = 2H$. Here we keep the notation in terms of H for traditional reasons. The δ term in Eq. (2) guarantees that the correlations converge in the limit $t_1 = t_2$. The above functional form $\langle \xi_H(t_1)\xi_H(t_2) \rangle = f(|t_1-t_2|)$ demonstrates that fractional Gaussian noise is a stationary process. When $2H < 1$ the noise correlator has a negative sign (antipersistence), while positive correlations (persistence) occur for $2H > 1$. Normal Brownian noise without correlations corresponds to the limit $H = 1/2$ and $H = 1$ is the limiting case of ballistic (fully persistent) motion.

A. Fractional Langevin equation

Fractional Langevin equations [35] are based on the generalized Langevin equation with power-law memory kernel. Generalized Langevin equations were particularly promoted by the work of Kubo [32] and have become a standard tool to describe complex diffusion dynamics. In particular, FLEs have been applied to model the internal dynamics of single protein molecules [36,37] or to describe diffusion in a viscoelastic continuum [25]. Fractional Langevin equations were analyzed in the framework of heat bath models in Ref. [38]. The discussion of some properties of FLE processes remains hypothetical. In particular, in the context of small-scale internal cell dynamics, the temporal resolution of single-particle tracking experiments is often above the threshold to detect ballistic motion. Many of the effects that can be theoretically derived or captured by simulations have yet to be experimentally confirmed. Nonetheless, this discussion is crucial since many aspects of FLE motion are in stark contrast to other models of anomalous diffusion, such as FBM and CTRWs, as we show below. Considering that the FLE can be derived under very general conditions (see, for example, Refs. [32,38]), we are confident that our results are applicable to a wide range of physical systems.

Without an external potential, the free FLE for the time dependence of the position coordinate $y(t)$ reads

$$m \frac{d^2}{dt^2} y(t) = -\bar{\gamma} \int_0^t (t-\tau)^{2H-2} \frac{dy}{d\tau}(\tau) d\tau + \eta \xi_H(t), \quad (3)$$

valid for persistent Hurst exponents $1/2 < H < 1$. Here m denotes the mass of the diffusing particle, $\bar{\gamma}$ is a generalized friction constant, η is the noise strength, and ξ_H is the fractional Gaussian noise. Further, η and $\bar{\gamma}$ are related by the fluctuation-dissipation theorem [32]

$$\eta = \sqrt{\frac{k_B T \bar{\gamma}}{2D_H H(2H-1)}}, \quad (4)$$

where $k_B T$ denotes thermal energy. Note that the power-law tail of the fractional Gaussian noise (2) is matched by the power-law kernel inside the memory integral expression of the FLE (3). For this power-law form we may rewrite the FLE as

$$m \frac{d^2}{dt^2} y(t) = -\bar{\gamma} \Gamma(2H-1) {}_0^C D_t^{2-2H} y(t) + \eta \xi(t), \quad (5)$$

where the fractional operator ${}_0^C D_t^{2-2H}$ in the Caputo sense is defined by comparison with Eq. (3). Introducing dimensionless quantities, one can show that the only free parameter of Eq. (3) is the initial velocity v_0 in units of the thermal velocity $\sqrt{k_B T/m}$, as can also be seen from the full solution (B2a).

In the presence of an external harmonic potential $V(x) = \frac{1}{2} \lambda x^2$, the FLE assumes the form

$$m \frac{d^2}{dt^2} y(t) = -\bar{\gamma} \int_0^t (t-\tau)^{2H-2} \frac{dy}{d\tau} d\tau + \eta \xi_H(t) - \lambda y(t), \quad (6)$$

with the Hookean restoring force term $\lambda y(t)$. Neglecting the left-hand side of this equation, we reach the overdamped limit. Kou applied this overdamped FLE to the movements of ligands within a single protein molecule [36] and provided the equilibrium solution to this equation.

B. Fractional Brownian motion

An alternative combination of fractional Gaussian noise and the particle position x is provided by the stochastic differential equation

$$\frac{dx(t)}{dt} = \xi_H(t). \quad (7)$$

This FBM was introduced by Kolmogorov [39] and became famous following the work of Mandelbrot and van Ness [33]. Further analysis in terms of the stochastic formulation and the ergodicity of the process is found in Refs. [20–22]. In the FBM model, the potential is directly added to the derivative process of FBM. In the case of a Hookean force of strength λ the stochastic equation becomes

$$\frac{dx(t)}{dt} = \xi_H(t) - \lambda x(t). \quad (8)$$

Note that despite the seemingly simple structure of Eqs. (7) and (8) FBM is a strongly non-Markovian process and cannot be mapped onto a random-walk process [40].

III. FREE FRACTIONAL LANGEVIN-EQUATION MOTION AND AGING BEHAVIOR

In this and the following sections we present the solutions for the ensemble- and time-averaged MSDs of the FLE and FBM processes introduced here and investigate their aging

behavior. Solutions to the FLE share many general properties with FBM on longer time scales, but due to their formulation in phase (velocity and position) space have differentiable trajectories [20,41]. We find that the aging of FBM and FLE is significantly different. Remarkably, the aging of the FLE varies between the cases of free and confined motion.

A. Ensemble-averaged moments

The free FLE has been widely used in literature (see, for example, Refs. [24,25,35]) and an equilibrium solution was provided by Pottier [41]. Here we extend this solution to nonequilibrium initial conditions v_0 analogous to Deng and Barkai [20]. From the two-point correlator, corresponding to the fluctuation $[\xi(t)]$ average of Eq. (3) shown in Appendix B we obtain the second moment

$$\begin{aligned} \langle y^2(t) \rangle &= 2 \frac{k_B T}{m} t^2 E_{2H,3}(-\gamma t^{2H}) \\ &+ \left(v_0^2 - \frac{k_B T}{m} \right) t^2 E_{2H,2}(-\gamma t^{2H}), \end{aligned} \quad (9)$$

with $\gamma = \bar{\gamma} \Gamma(2H-1)/m$. The generalized Mittag-Leffler function $E_{\alpha,\beta}$ has the series expansions [42]

$$E_{\kappa,\rho}(z) = \sum_{n=0}^{\infty} \frac{z^n}{\Gamma(\rho + \kappa n)} \quad (10a)$$

and

$$E_{\kappa,\rho}(z) = - \sum_{n=1}^{\infty} \frac{z^{-n}}{\Gamma(\rho - \kappa n)} \quad (10b)$$

around $z = 0$ and $|z| = \infty$, respectively. The free FLE process thus exhibits a characteristic crossover from ballistic motion

$$\langle y^2(t) \rangle \sim v_0^2 t^2 \quad (11)$$

to subdiffusion (note that $H > 1/2$)

$$\langle y^2(t) \rangle \sim \frac{2}{\gamma} \langle v^2 \rangle_{\text{th}} \frac{t^{2-2H}}{\Gamma(3-2H)}, \quad (12)$$

where the thermal squared velocity is given by $\langle v^2 \rangle_{\text{th}} = k_B T/m$. With the anomalous diffusion constant $D_H = \langle v^2 \rangle_{\text{th}} / [\gamma \Gamma(3-2H)]$ we rewrite the latter result in the more convenient form

$$\langle y^2(t) \rangle \sim 2D_H t^{2-2H}. \quad (13)$$

This result demonstrates that for FLE motion persistent (positively correlated) fractional Gaussian noise affects subdiffusion, in contrast to the case of FBM shown below. The result (9) and the asymptotic behaviors (11) and (12) are shown in Fig. 1, with excellent agreement between theory and stochastic simulations. The crossover between initial ballistic motion and terminal subdiffusion defines the intrinsic time scale $\tau = \gamma^{-1/(2H)}$. Note that in the highly specialized case of vanishing initial velocity the ballistic motion is replaced by an initial hyperdiffusive regime

$$\langle y^2(t) \rangle \sim 2(2H+1)\gamma \langle v^2 \rangle_{\text{th}} \frac{t^{2+2H}}{\Gamma(3+2H)}, \quad (14)$$

which is also shown in Fig. 1. The possibility of such a superballistic diffusion for Langevin-equation models with

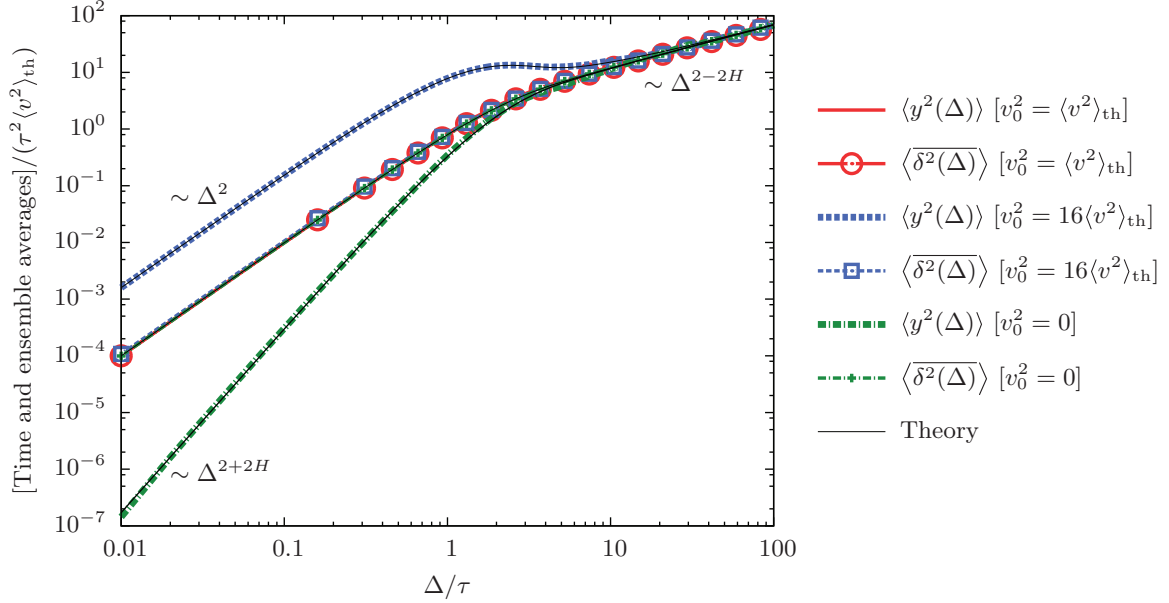


FIG. 1. (Color online) Ensemble- and time-averaged MSDs for free FLE motion with different initial velocities v_0 . The solid lines represent the theoretical results (9) and (20). The equilibrium MSD and the time-averaged MSDs coincide. The ensemble averages for the nonequilibrium processes approach the time averages at long times Δ . All simulations are performed with $h = 0.01$ (see Appendix A), $H = 0.625$, $t_a = 0$, and $T/\tau = 100$. Ensemble averages contain 1000 trajectories.

vanishing initial velocities was reported in Refs. [43,44], showing that superballistic diffusion may occur due to the high amount of energy that the particle gains during equilibration. Notably, this effect occurs even for a Brownian particle ($H = 1/2$). Experimentally, such a state may, for instance, be prepared by trapping the particle in a highly focused optical tweezers trap, which is switched off at $t = 0$.

According to Eq. (9), the mean-squared position of the free FLE process has a nonequilibrium contribution that is proportional to the difference $v_0^2 - \langle v^2 \rangle_{\text{th}}$ between the initial and the thermal kinetic energy. This contribution vanishes algebraically at long times, mirroring the equilibration but also the aging of the process (discussed below).

The first moment of y ,

$$\langle y(t) \rangle = v_0 t E_{2H,2}(-\gamma t^{2H}), \quad (15)$$

has the asymptotic behavior

$$\langle y(t) \rangle \sim v_0 t \quad (16)$$

at short times and, terminally,

$$\langle y(t) \rangle \sim \frac{v_0}{\gamma \Gamma(2-2H)} t^{1-2H}. \quad (17)$$

It thus approaches zero at long times since the equilibrated process is symmetric. Intriguingly, the approach to the steady state becomes slower when the Hurst parameter tends to $1/2$. The Brownian case $H = 1/2$ itself equilibrates exponentially and at long times has the thermal first moment of $\lim_{t \rightarrow \infty} \langle y(t) \rangle = v_0/\gamma$. This property can be interpreted as follows: The Brownian particle starting with an initial velocity will keep this velocity for a while until the friction slows it down on the characteristic length scale v_0/γ . Afterward, the particle diffuses symmetrically around this stalling point. A free FLE particle with its coupled power-law forms of the

noise correlations and the friction kernel does not feature this property and will on long time scales diffuse around the original starting point.

Combining the second and first moments, we obtain the variance $\langle y^2(t) \rangle - \langle y(t) \rangle^2$. At short times, this quantity is independent of the initial velocity v_0 and exhibits precisely the hyperdiffusive behavior (14). At longer times, due to the thermalization of the velocity, the asymptotic behavior of $\langle [\Delta y(t)]^2 \rangle$ follows expression (13).

An additional feature of the FLE process is distinct oscillations in the MSD, as shown in Fig. 2. These were reported before [22,45] and appear for a large Hurst index; they occur for all possible initial conditions in both the ensemble- and time-averaged MSDs. For which values of the Hurst parameter H are these oscillations possible? The derivative of Eq. (9) shows that the equilibrium MSD of the free FLE only has extrema and thus oscillates if the function $E_{2H,2}(-\gamma t^{2H})$ has zeros. Numerical analysis demonstrates that this condition is met for $H \gtrsim 0.8 \pm 10^{-4}$. Remarkably, this critical Hurst parameter for oscillations is preserved under nonequilibrium initial conditions.

B. Time-averaged mean-squared displacement and aging

From the exact results for the second moment $\langle y^2(t) \rangle$ and the autocorrelation function $\langle y(t_1)y(t_2) \rangle$ we obtain the time-averaged MSD through

$$\begin{aligned} \overline{\langle \delta^2(\Delta) \rangle} &= \frac{1}{T-\Delta} \int_{t_a}^{t_a+T-\Delta} [\langle x^2(t'+\Delta) \rangle + \langle x^2(t') \rangle \\ &\quad - 2\langle x(t'+\Delta)x(t') \rangle] dt'. \end{aligned} \quad (18)$$

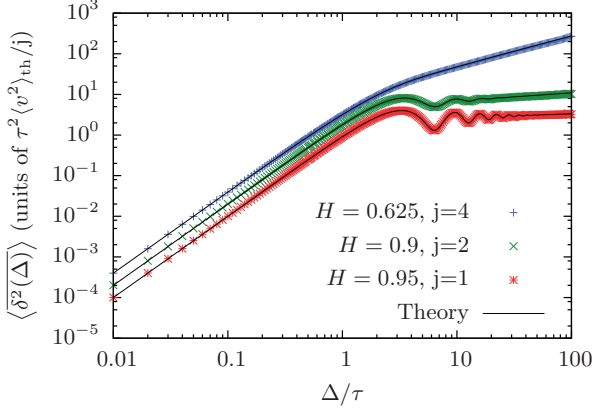


FIG. 2. (Color online) For large Hurst parameters $H > 0.8$, oscillations occur in the MSD of the free FLE. These oscillations are more pronounced for larger H . The data are simulated for different Hurst parameters with initial velocities $v_0^2 = \langle v^2 \rangle_{\text{th}}$, $h = 0.01$ (see Appendix A), and $T/\tau = 100$ and for 1000 trajectories. The theoretical values are calculated according to Eq. (20). For better visibility, the plots are shifted by the factor j along the logarithmic ordinate.

Based on the full solution (B2a) for the free FLE, we find that $\overline{\delta^2(\Delta)}$ splits into two additive contributions

$$\overline{\delta^2(\Delta)} = f_{\text{st}}(\Delta) + f_{\text{age}}(\Delta; t_a, T). \quad (19)$$

In contrast to CTRW subdiffusion, the time-averaged MSD of the free FLE motion does not vanish for long measurement and aging times T and t_a , respectively. Namely, it has a stationary contribution f_{st} that only depends on the lag time Δ . All dependences on t_a or T are captured by the aging term f_{age} , which decays for long T and t_a . We will obtain an analogous behavior for the FLE in a harmonic potential and FBM below.

The stationary contribution for the free FLE becomes

$$f_{\text{st}} = 2\langle v^2 \rangle_{\text{th}} \Delta^2 E_{2H,3}(-\gamma \Delta^{2H}), \quad (20)$$

with a crossover from the ballistic short-time expansion

$$f_{\text{st}} \sim \frac{2\langle v^2 \rangle_{\text{th}} \Delta^2}{\Gamma(2H)} \quad (21)$$

to the asymptotic subdiffusive form

$$f_{\text{st}} \sim \frac{2\langle v^2 \rangle_{\text{th}}}{\gamma \Gamma(2H - 2)} \Delta^{2-2H}. \quad (22)$$

For the aging term the following expression holds:

$$f_{\text{age}} = \frac{v_0^2 - \langle v^2 \rangle_{\text{th}}}{T - \Delta} \int_{t_a}^{t_a + T - \Delta} \{(t + \Delta) E_{2H,2}[-\gamma(t + \Delta)^{2H}] - t E_{2H,2}[-\gamma t^{2H}]\}^2 dt, \quad (23)$$

which vanishes when the initial velocity has the value of the thermal velocity $\pm \langle v^2 \rangle_{\text{th}}^{1/2}$. The term in the integral is always positive and at long t has the asymptotic form

$$[\dots]^2 \sim \frac{\Delta^2}{\gamma^2 \Gamma^2(1 - 2H)} t^{-4H} \quad (24)$$

such that due to $H > 1/2$ it is integrable. We can further approximate the aging term in the experimentally relevant

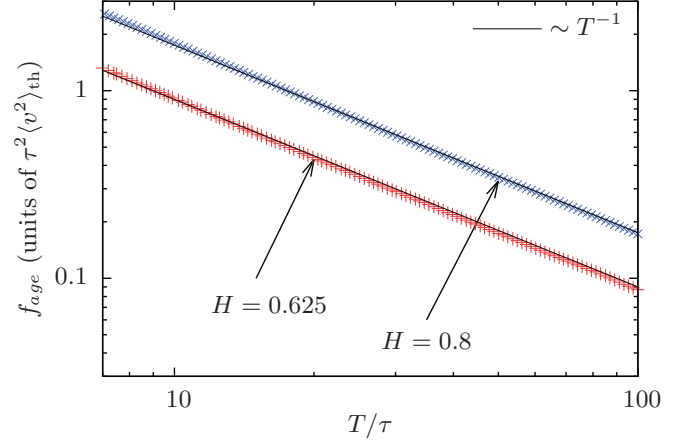


FIG. 3. (Color online) Measurement time T dependence of the free FLE, confirming the proportionality to $1/T$. Here f_{age} is calculated by subtracting the theoretical results for f_{st} (20) from the simulated values for the time-averaged MSD. The simulations are run with $h = 0.01$ (see Appendix A), $v_0^2 = 100\langle v^2 \rangle_{\text{th}}$, $\Delta/\tau = 0.5$, and $t_a = 0$ and are averaged over 1000 trajectories.

regime. For evaluating time averages it is crucial to have sufficiently long time series, i.e., the collected data should be extensive enough to produce reliable statistics. This means that we will observe the limit $T \gg \Delta$. Additionally, we assume the intrinsic time scale to be very short in comparison to accessible measurement times, i.e., we take the limit $T \gg \tau$. Finally, we keep the aging time finite, i.e., $T \gg t_a$. In these limits, the integral will approach a finite value $\overline{\tau}_{\infty}(\Delta, t_a)$ due to the above convergence criterion. We thus identify the long- T dependence

$$f_{\text{age}} = [v_0^2 - \langle v^2 \rangle_{\text{th}}] \frac{\overline{\tau}_{\infty}(\Delta, t_a)}{T} + O(\gamma^{-2} T^{-4H}). \quad (25)$$

The $1/T$ scaling of the aging contribution f_{age} is demonstrated in comparison with simulation results in Fig. 3. For $T \rightarrow \infty$ only the stationary term of $\overline{\delta^2(\Delta)}$ remains and in that limit we find the ergodic behavior

$$\overline{\delta^2(\Delta)} = \lim_{t \rightarrow \infty} \langle [y(t + \Delta) - y(t)]^2 \rangle = \langle y^2(\Delta) \rangle \quad (26)$$

under the condition that the initial velocity is thermalized $v_0^2 = \langle v^2 \rangle_{\text{th}}$, consistent with the results of Ref. [20].

What happens when the process is strongly aged? In the associated limit of $t_a \gg \Delta$ and $t_a \gg \gamma^{-1/(2H)}$ as well as $T \gg \Delta$ we obtain

$$f_{\text{age}} = \frac{(v_0^2 - \langle v^2 \rangle_{\text{th}}) \Delta^2}{(1 - 4H) \gamma^2 \Gamma^2(1 - 2H)} \frac{(T + t_a)^{1-4H} - t_a^{1-4H}}{T}. \quad (27)$$

If additionally $t_a \gg T$, we thus find the scaling

$$f_{\text{age}} \sim \frac{(v_0^2 - \langle v^2 \rangle_{\text{th}}) \Delta^2}{\gamma^2 \Gamma^2(1 - 2H)} t_a^{-4H}. \quad (28)$$

This asymptotic dependence on the aging time t_a is illustrated in Fig. 4. The above results show that the relaxation of the aging dependence becomes slower when H approaches the Brownian value $H = 1/2$.

Remarkably, the first-order correction for highly aged systems is quadratic in the lag time Δ . Hence the coefficient for the ballistic regime in Eq. (20) could potentially be

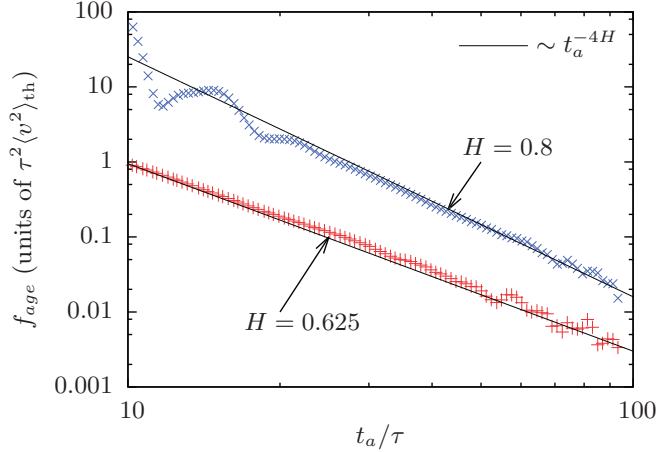


FIG. 4. (Color online) Aging time dependence of the free FLE motion, recovering the proportionality to t_a^{-4H} . The parameters are $h = 0.01$ (see Appendix A), $\Delta/\tau = 0.5$, and $T/\tau = 5$, so that the data are in the limit $t_a \gg T \gg \Delta$. For $H = 0.625$, the initial velocity is $v_0^2 = 4 \times 10^4 \langle v^2 \rangle_{th}$ and the number of trajectories is 10 000. For $H = 0.8$, the initial velocity is $v_0^2 = 25 \times 10^4 \langle v^2 \rangle_{th}$ and the number of trajectories is 10^5 . The simulated values for $H = 0.8$ are multiplied by a constant factor of 10 for visual convenience.

overestimated or underestimated if it is gained from aged particle trajectories.

IV. CONFINED FRACTIONAL LANGEVIN-EQUATION MOTION AND AGING BEHAVIOR

We now turn to the FLE (6) in the presence of a confining, external harmonic potential and analyze the dynamics in terms of the ensemble- and time-averaged MSDs. In particular, we find the remarkable result that the aging behavior is different from the free FLE motion. In experiments, a harmonic potential could, for example, be generated by an optical tweezers. We can also interpret the harmonic potential as an approximation to other systems, for example, a particle in a “soft box” such as a compartment inside a biological cell. For such systems, we expect our results to be conserved qualitatively.

A. Ensemble-averaged moments

In the underdamped case [i.e., keeping the inertial term on the left-hand side of Eq. (6)], the second moment of the position can be written in the form (compare Appendix B)

$$\langle y^2(t) \rangle = \langle y^2 \rangle_{th} + (y_0^2 - \langle y^2 \rangle_{th})A^2(t) + (v_0^2 - \langle v^2 \rangle_{th})B^2(t) + 2y_0v_0A(t)B(t), \quad (29)$$

where $\langle y^2 \rangle_{th} = k_B T / \lambda$ is the thermal value of the position coordinate and $A(t)$ and $B(t)$ are defined via their Laplace transforms (s denoting the Laplace variable) through

$$A(s) = \frac{\gamma s^{1-2H} + ms}{ms^2 + \gamma s^{2-2H} + \lambda}, \quad (30a)$$

$$B(s) = \frac{m}{ms^2 + \gamma s^{2-2H} + \lambda}. \quad (30b)$$

The thermal value of the second moment $\langle y^2 \rangle_{th} = \int y^2 P_{th}(y) dy$ involves spatial averaging over an equilibrium probability density $P_{th}(y) = \lim_{t \rightarrow \infty} P(y, t)$. Analogously, the thermal ensemble MSD $\langle [y(\Delta) - y(0)]^2 \rangle_{th} = \lim_{t \rightarrow \infty} \langle [y(t + \Delta) - y(t)]^2 \rangle$ can be obtained through the spatial correlation function $\langle y(0 + \Delta)y(0) \rangle_{th}$ (see Appendix B): $\langle [y(\Delta) - y(0)]^2 \rangle_{th} = 2\langle y^2 \rangle_{th} - 2\langle y(\Delta)y(0) \rangle_{th} = 2\langle y^2 \rangle_{th}[1 - A(\Delta)]$.

In the overdamped case, which was discussed in Ref. [36], we obtain the simpler result

$$\langle y^2(t) \rangle = \langle y^2 \rangle_{th} + (y_0^2 - \langle y^2 \rangle_{th})E_{2-2H}^2 \left(-\frac{\lambda}{\gamma} t^{2-2H} \right), \quad (31)$$

with $\gamma = \bar{\gamma}\Gamma(2H - 1)$. Here $E_\alpha = E_{\alpha,1}$ is the regular Mittag-Leffler function. At short times we observe the leading-order behavior

$$\langle y^2(t) \rangle \sim y_0^2 - \frac{2\lambda(y_0^2 - \langle y^2 \rangle_{th})}{\gamma\Gamma(3-2H)} t^{2-2H}. \quad (32)$$

That is, starting from the initial value y_0^2 we have a decay or increase of $\langle y^2(t) \rangle$ depending on the sign of $y_0^2 - \langle y^2 \rangle_{th}$. Asymptotically the second moment exhibits the power-law convergence

$$\langle y^2(t) \rangle \sim \langle y^2 \rangle_{th} + (y_0^2 - \langle y^2 \rangle_{th}) \frac{\gamma^2}{\lambda^2} \frac{t^{4H-4}}{\Gamma^2(2H-1)} \quad (33)$$

to the thermal value $\langle y^2 \rangle_{th} = k_B T / \lambda$. The approach to this thermal value is from above when $y_0^2 > \langle y^2 \rangle_{th}$ and from below in the opposite case. This relaxation occurs on the intrinsic time scale $\tau = (\gamma/\lambda)^{1/(2-2H)}$. The above behavior is shown in Fig. 5. We note that in terms of dimensionless variables Eq. (29) has two free parameters: the rescaled initial velocity and the initial position. In the overdamped case only the initial position is relevant [see also the full solutions (B2b) and (B2c)].

The first moment of the confined FLE motion is given by the relaxation pattern

$$\langle y(t) \rangle = A(t)y_0 + B(t)v_0 \quad (34)$$

for the full solution and, in the overdamped case, by the Mittag-Leffler form

$$\langle y(t) \rangle = y_0 E_{2-2H} \left(-\frac{\lambda}{\gamma} t^{2-2H} \right) \quad (35)$$

with the asymptotic behavior

$$\langle y(t) \rangle \sim \frac{y_0 \gamma}{\gamma\Gamma(2H-1)} t^{2H-2}. \quad (36)$$

B. Time-averaged mean-squared displacement and aging

The full solution for the time-averaged MSD $\overline{\langle \delta^2(\Delta) \rangle}$ is additive as in Eq. (19) with the following two contributions. The stationary term reads

$$f_{st} = 2\langle y^2 \rangle_{th}[1 - A(\Delta)] \quad (37)$$

in the underdamped case and

$$f_{st} = 2\langle y^2 \rangle_{th} \left[1 - E_{2-2H} \left(-\frac{\lambda}{\gamma} \Delta^{2-2H} \right) \right] \quad (38)$$

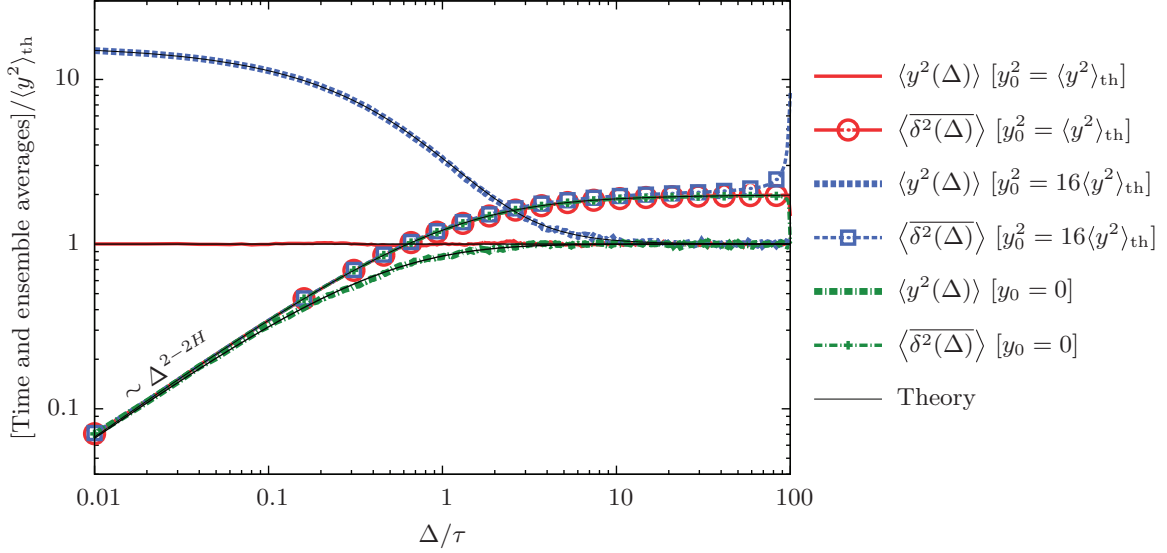


FIG. 5. (Color online) Ensemble-averaged and time-averaged MSDs for the overdamped FLE motion in a confining, external harmonic potential for $H = 0.625$. The simulations are performed with the parameter values $t_a = 0$, $T/\tau = 100$, and $h = 0.01$ (see Appendix A) and are averaged over 10^4 trajectories. The theoretical behavior is provided by Eqs. (31) and (38). We observe excellent agreement between theory and simulation. In accordance with Ref. [22], the time averages approach twice the value of the ensemble averages. For large Δ , Eq. (38) breaks down since it is valid only in the limit $T \gg \Delta$. Instead, we have $\langle \delta^2(\Delta = T) \rangle = \langle [y(T) - y(0)]^2 \rangle = \langle y^2 \rangle_{\text{th}} + y_0^2$.

in the overdamped case. The latter turns over from the subdiffusive short-lag-time growth

$$f_{\text{st}} \sim 2\langle y^2 \rangle_{\text{th}} \frac{\lambda}{\gamma} \frac{\Delta^{2-2H}}{\Gamma(3-2H)} \quad (39)$$

to the asymptotic long- Δ approach

$$f_{\text{st}} \sim 2\langle y^2 \rangle_{\text{th}} \left[1 - \frac{\gamma}{\lambda} \frac{\Delta^{2H-2}}{\Gamma(2H-1)} \right] \quad (40)$$

to twice the thermal value $\langle y^2 \rangle_{\text{th}}$. This factor of 2 stems from the very definition of the time-averaged MSD (1) [compare Eq. (18) [22]].

The aging term becomes

$$\begin{aligned} f_{\text{age}} &= \frac{y_0^2 - \langle y^2 \rangle_{\text{th}}}{T - \Delta} \int_{t_a}^{t_a+T-\Delta} [A(t+\Delta) - A(t)]^2 dt \\ &+ \frac{v_0^2 - \langle v^2 \rangle_{\text{th}}}{T - \Delta} \int_{t_a}^{t_a+T-\Delta} [B(t+\Delta) - B(t)]^2 dt \\ &+ \frac{2y_0v_0}{T - \Delta} \int_{t_a}^{t_a+T-\Delta} [A(t+\Delta) - A(t)] \\ &\times [B(t+\Delta) - B(t)] dt, \end{aligned} \quad (41)$$

which can be used for numerical evaluation. In the overdamped case, this expression simplifies to

$$\begin{aligned} f_{\text{age}} &= \frac{y_0^2 - \langle y^2 \rangle_{\text{th}}}{T - \Delta} \int_{t_a}^{t_a+T-\Delta} \left[E_{2-2H} \left(-\frac{\lambda}{\gamma} (t+\Delta)^{2-2H} \right) \right. \\ &\left. - E_{2-2H} \left(-\frac{\lambda}{\gamma} t^{2-2H} \right) \right]^2 dt. \end{aligned} \quad (42)$$

For $t \gg \Delta$ the integrand in the above expression decays like

$$\begin{aligned} [\dots]^2 &\sim \frac{\lambda^2}{\gamma^2} \Delta^2 t^{2-4H} E_{2-2H, 2-2H} \left(-\frac{\lambda}{\gamma} t^{2-2H} \right) \\ &\sim \frac{\gamma^2}{\lambda^2 \Gamma^2(2-2H)} \Delta^2 t^{4H-6}, \end{aligned} \quad (43)$$

where the second approximation holds when, in addition, $t \gg \tau$. As the exponent $4H - 6$ ranges in the interval between -2 and -4 , the integral converges and approaches the finite value $\mathbb{T}_{\infty}(\Delta, t_a)$, which increases with t_a . For $T \gg \Delta, \tau, t_a$ we thus find

$$f_{\text{age}} \sim (y_0^2 - \langle y^2 \rangle_{\text{th}}) \frac{\mathbb{T}_{\infty}(\Delta, t_a)}{T}. \quad (44)$$

This $1/T$ dependence on the process time T is in good agreement with our simulations, as demonstrated in Fig. 6.

In the aging limit $t_a \gg \Delta$, $t_a \gg \tau$, and $T \gg \Delta$ we find the asymptotic behavior

$$f_{\text{age}} \sim \frac{(y_0^2 - \langle y^2 \rangle_{\text{th}}) \gamma^2}{(4H-5) \lambda^2 \Gamma^2(2-2H)} \Delta^2 \frac{(T+t_a)^{4H-5} - t_a^{4H-5}}{T}. \quad (45)$$

If we assume strong aging in the sense $t_a \gg T$, we arrive at the scaling behavior

$$f_{\text{age}} \sim \frac{(y_0^2 - \langle y^2 \rangle_{\text{th}}) \gamma^2}{\lambda^2 \Gamma^2(2-2H)} \Delta^2 t_a^{4H-6}. \quad (46)$$

This prediction is confirmed in Fig. 7. Note the difference to the t_a scaling (28) of the free FLE motion. Remarkably, the aging terms for overdamped and underdamped FLEs under confinement coincide in the considered limits.

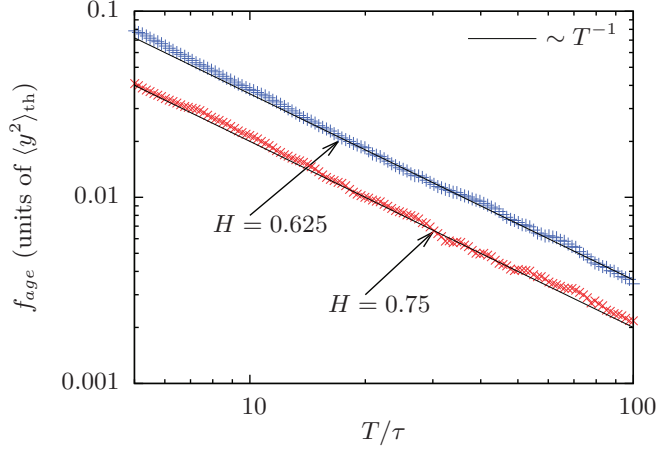


FIG. 6. (Color online) Measurement time T dependence of the overdamped confined FLE process showing the predicted T^{-1} decay. Here f_{age} is obtained by subtracting the theoretical value of f_{st} from the time-averaged MSD. The simulations are performed for $y_0^2 = 16\langle y^2 \rangle_{\text{th}}$, $h = 0.01$ (see Appendix A), $\Delta/\tau = 0.3$, and $t_a = 0$ and are averaged over 10^4 trajectories.

V. FRACTIONAL BROWNIAN MOTION

We now turn to FBM, in which the fractional Gaussian noise is external. Therefore, when we consider the ensemble-averaged MSD of free FBM,

$$\langle x^2(t) \rangle = 2D_H t^{2H}, \quad (47)$$

we see that antipersistent noise with $0 < H < 1/2$ corresponds to subdiffusion, in contrast to FLE motion, where the noise is counterweighted by the friction kernel. Here we calculate the

dynamic quantities for confined FBM described by Eq. (8). This derivation is analogous to Ref. [22].

A. Ensemble-averaged moments

As this process does not fulfill Kubo's fluctuation-dissipation theorem, it does not have a solution that starts in equilibrium. If one extends the solution of Ref. [22] to nonzero initial conditions one obtains the second moments listed in Appendix B. The ensemble-averaged MSD yields

$$\begin{aligned} \langle x^2(t) \rangle = & x_0^2 e^{-2\lambda t} + \frac{D_H}{\lambda^{2H}} \gamma(2H + 1, \lambda t) + 2D_H e^{-\lambda t} t^{2H} \\ & - \frac{\lambda D_H}{2H + 1} e^{-2\lambda t} t^{2H+1} M(2H + 1, 2H + 2, \lambda t). \end{aligned} \quad (48)$$

Here γ is the lower incomplete gamma function and M denotes the Kummer function [46]. Functional Brownian motion in an harmonic external potential has an intrinsic time scale of $\tau = 1/\lambda$ (see Fig. 8). Rescaling of the dynamic equation for the confined FBM (8) reveals that the only free parameter is the initial position.

At short times we obtain the behavior

$$\langle x^2(t) \rangle \sim x_0^2 - 2\lambda x_0^2 t + 2D_H t^{2H}. \quad (49)$$

For the case $H < 1/2$ the fractional term dominates and for $H > 1/2$ the linear term dominates. Counterintuitively, the process exhibits overshooting, i.e., local maxima in the MSD, for the subdiffusive case $H < 1/2$ (not shown). In the limit $\lambda = 0$ we recover the ensemble-averaged MSD (47) of free FBM. With the asymptotic expansions

$$M(2H + 1, 2H + 2, z) \sim \frac{2H + 1}{z} e^{-z} \quad (50)$$

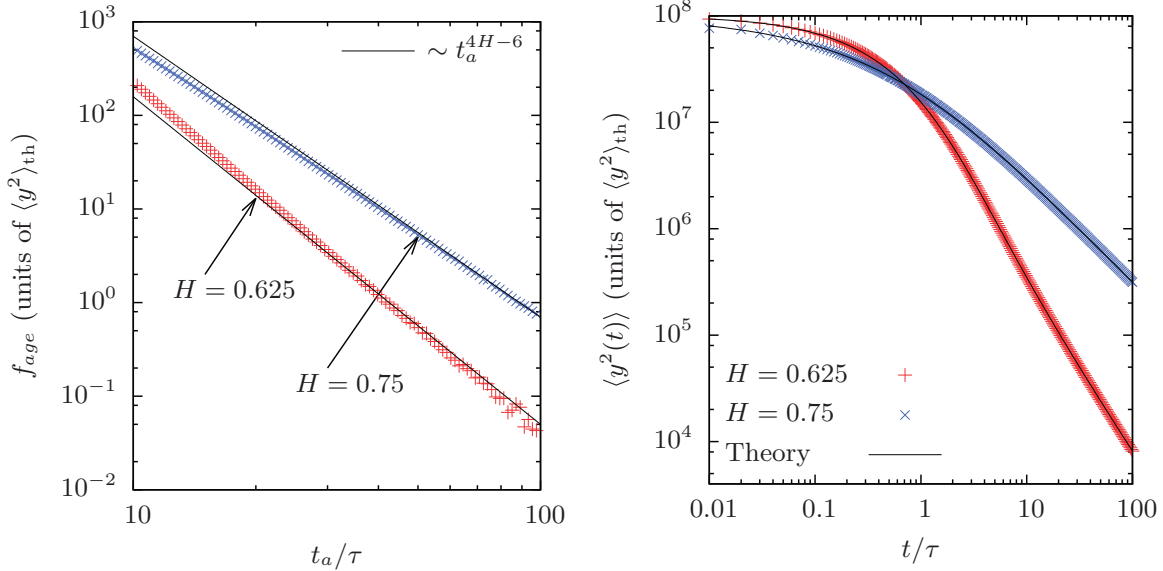


FIG. 7. (Color online) Plotted on the left is the aging dependence on t_a of the overdamped confined FLE process. The simulations use $y_0^2 = 10^8 \langle y^2 \rangle_{\text{th}}$ and $h = 0.01$ (see Appendix A) and the values are averaged over 10^4 trajectories. We choose $\Delta/\tau = 0.3$ and $T/\tau = 0.4$ to guarantee the limit $t_a \gg \Delta, T$. In order to validate that the linearization in the simulation scheme is accurate for this particular h and the comparatively high starting kinetic energies, the mean-squared position is plotted on the right and compared to the theoretical result (31), observing excellent agreement.

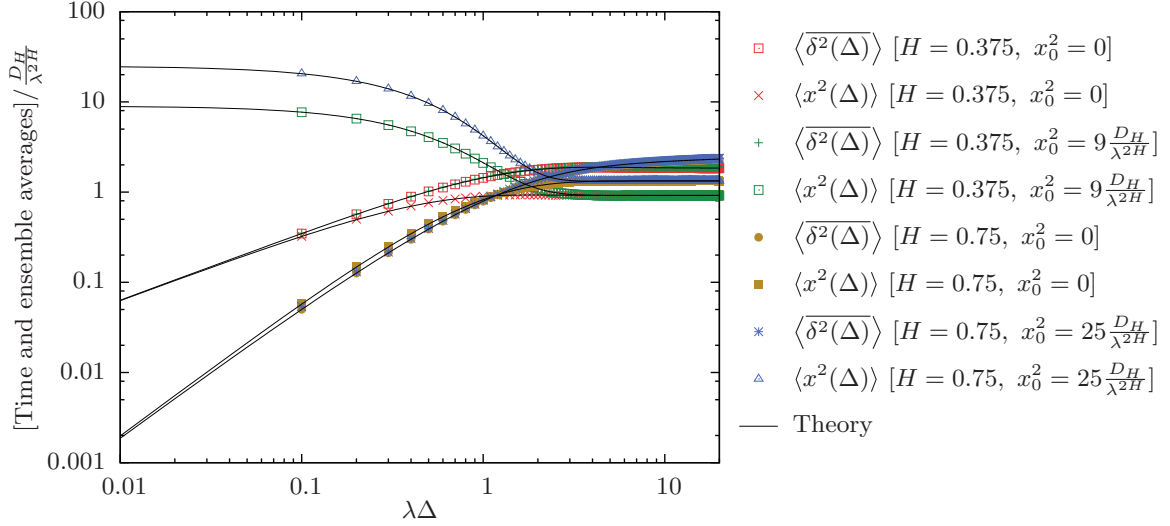


FIG. 8. (Color online) Time- and ensemble-averaged MSDs (55) and (48) for confined FBM with the indicated parameters. We observe excellent agreement between theory and simulation. For a fixed Hurst parameter, the time-averaged MSD approaches twice the stationary value $\langle x^2 \rangle_{\text{th}}$. The stationary values depend on the Hurst parameter H (see Ref. [47]). The short-time behavior depends on the initial value x_0 . All simulations are run with $h = 0.1$ (see Appendix A), $T/\tau = 300$, and $t_a = 0$ and represent averages over 10^5 trajectories.

and

$$\gamma(2H + 1, z) \sim \Gamma(2H + 1) - z^{2H} e^{-z} \quad (51)$$

for the Kummer and incomplete γ functions, respectively, in the limit $t \gg \tau$ we find

$$\begin{aligned} \langle x^2(t) \rangle \sim & \frac{D_H \Gamma(2H + 1)}{\lambda^{2H}} + x_0^2 e^{-2\lambda t} \\ & - \frac{2}{\lambda^2} 2H(2H - 1) D_H t^{2H-2} e^{-\lambda t}. \end{aligned} \quad (52)$$

Thus, after an exponential relaxation with characteristic decay time $1/\lambda$ the system reaches the stationary value

$$\langle x^2 \rangle_{\text{st}} = D_H \Gamma(2H + 1) / \lambda^{2H}. \quad (53)$$

As the Kubo condition is missing for this process, the stationary value explicitly depends on the Hurst parameter H , thus demonstrating the nonequilibrium character. The activation as a function of H of the stationary value $\langle x^2 \rangle_{\text{st}}$ was demonstrated by simulations in Ref. [47]. For the first moment we find the exponential decay

$$\langle x(t) \rangle = x_0 e^{-\lambda t}. \quad (54)$$

B. Time-averaged mean-squared displacement and aging

From the explicit result for the time-averaged MSD $\overline{\langle \delta^2(\Delta) \rangle}$ in Eq. (C1) we see that also for this process we obtain the additive combination (19) of a stationary and an aging contribution. The stationary part is given by

$$\begin{aligned} f_{\text{st}} = & 2D_H \Delta^{2H} + \frac{2D_H}{\lambda^{2H}} \Gamma(2H + 1) \\ & - \frac{D_H}{\lambda^{2H}} [\Gamma(2H + 1, \lambda \Delta) e^{\lambda \Delta} + \Gamma(2H + 1) e^{-\lambda \Delta}] \\ & - \frac{D_H \lambda}{2H + 1} \Delta^{2H+1} e^{-\lambda \Delta} M(2H + 1; 2H + 2; \lambda \Delta), \end{aligned} \quad (55)$$

where $\Gamma(a, z)$ is the upper incomplete Gamma function. Interestingly, as discovered in Ref. [22], the approach to the stationary value of the time-averaged MSD is of power-law form

$$\begin{aligned} f_{\text{st}} \sim & \frac{2D_H \Gamma(2H + 1)}{\lambda^{2H}} - \frac{D_H}{\lambda^{2H}} \Gamma(2H + 1) e^{-\lambda \Delta} \\ & + \frac{4H(2H - 1) D_H}{\lambda^2} \Delta^{2H-2}, \end{aligned} \quad (56)$$

contrasting the exponentially fast relaxation of the ensemble MSD. Note again the factor of 2 in the stationary value due to the definition of $\overline{\langle \delta^2(\Delta) \rangle}$. We demonstrate in Figs. 9 and 10 that the measurement time dependence of the aging term is indeed of the form $f_{\text{age}} \simeq 1/T$ and that the aging time

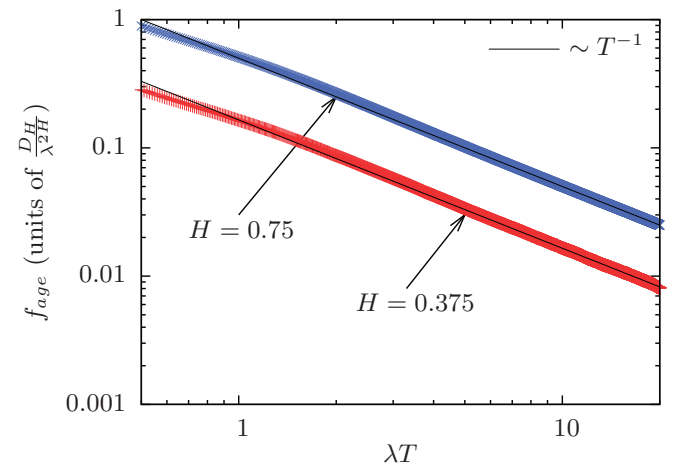


FIG. 9. (Color online) Measurement time T dependence for confined FBM, confirming the $1/T$ behavior. The simulation parameters are $h = 0.01$ (see Appendix A), $\Delta/\tau = 0.2$, and $t_a = 0$. The results are averaged over 10^5 trajectories. The simulation for $H = 0.75$ start with $x_0^2 = 25D_H/\lambda^{2H}$ and the one for $H = 0.375$ with $x_0^2 = 9D_H/\lambda^{2H}$.

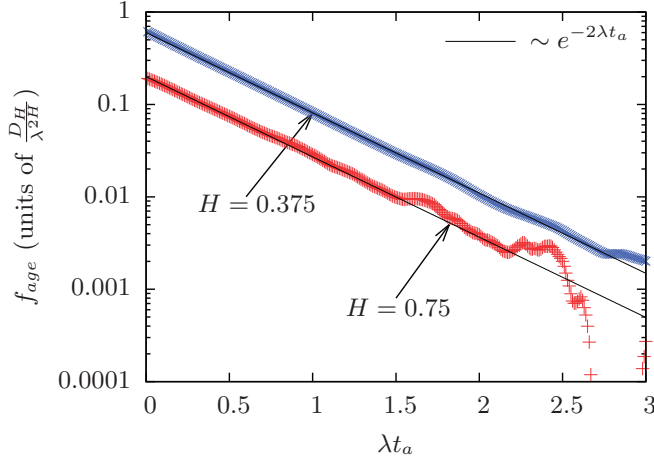


FIG. 10. (Color online) Aging for confined FBM, showing the predicted exponential decay (57). Simulations use $h = 0.01$ (see Appendix A) and $\Delta/\tau = 0.2$, averaging over 10^5 trajectories. The simulation for $H = 0.75$ start with $x_0^2 = 25D_H/\lambda^{2H}$ and the one for $H = 0.375$ with $x_0^2 = 9D_H/\lambda^{2H}$.

dependence is of the form

$$f_{\text{age}} \sim x_0^2 \exp(-2\lambda t_a). \quad (57)$$

Both relations can be shown analytically.

VI. DISCUSSION

We studied the FLE and FBM models for anomalous diffusion that is driven by fractional Gaussian noise. From the results for the ensemble-averaged first and second moments, we obtained the associated time-averaged MSD $\overline{\langle \delta^2(\Delta) \rangle}$. The exact expression for $\overline{\langle \delta^2(\Delta) \rangle}$ was shown to separate into two additive contributions, a stationary one and an aging term. The aging term vanishes inverse proportionally at large measurement times. While solutions to regular Langevin equations with white noise as well as the confined FBM show exponential relaxation of the time-averaged MSD in the aging time, solutions to FLEs exhibit power-law relaxation and power-law aging with a characteristic exponent between

-1 and -3 . Notably, the aging exponents differ between free and confined FLE motion.

The existence of the finite stationary term of the time-averaged MSD for stochastic processes driven by fractional Gaussian noise contrasts the properties of the CTRW process, for which the time-averaged MSD decays to zero in the respective limits. The origin of this difference is that a CTRW particle effectively grinds to a complete halt after a sufficiently long time, while a free FLE particle keeps spreading. Hence the aging dynamics in CTRWs and the free FLE are distinguishable. In particular, it should be noted that free FBM, which is equivalent to overdamped free FLE motion [20], does not exhibit aging at all.

What happens when, instead of fixed initial conditions v_0 , x_0 , and y_0 as well as aging times t_a we analyze an ensemble of trajectories with distributed aging times or initial conditions? In such cases our aging formulas may also be useful. Consider the example of free FLE motion. Let $\langle \cdot \rangle$ denote the ensemble average for a fixed aging time t_a and a fixed initial condition v_0 . Let $\langle \cdot \rangle_{\text{dis}}$ denote the ensemble average over trajectories with distributed aging times t_a and initial velocities v_0 and let P denote the probability for a given value of v_0 and t_a . Then we obtain

$$\overline{\langle \delta^2(\Delta) \rangle}_{\text{dis}} = \int_0^\infty dt_a \int_{-\infty}^\infty dv_0 \overline{\langle \delta^2(\Delta; t_a, v_0) \rangle} P(t_a, v_0). \quad (58)$$

Hence the time-averaged MSD over an ensemble of trajectories with distributed initial conditions and aging times can be calculated by weighting our result for the time-averaged MSD for fixed t_a and v_0 with the probability for that aging time and initial condition to occur $P(t_a, v_0)$. This probability will eventually depend on the experimental setup.

ACKNOWLEDGMENTS

Financial support from the Engineering and Physical Sciences Research Council, the Academy of Finland (FiDiPro scheme), and the CompInt graduate school at TUM is gratefully acknowledged. R.M. thanks the Mathematical Institute of the University of Oxford for financial support through an OCCAM Visiting Fellowship.

APPENDIX A: SIMULATION SCHEMES

The simulation schemes for the stochastic differential equations are based on the method originally proposed by Deng and Barkai [20] and also used in Ref. [21]. In order to derive the scheme, we first integrate the dynamic equations (3), (6), and (8) over time. This leads to

$$mv(t) = mv_0 - \frac{\bar{v}}{2H-1} \int_0^t (t-\tau)^{2H-1} v(\tau) d\tau + \eta B_H(t) \quad (A1)$$

for the free FLE,

$$\lambda \int_0^t y(\tau) d\tau = -\bar{y} \int_0^t (t-\tau)^{2H-2} y(\tau) d\tau + \frac{\bar{y} y_0}{2H-1} t^{2H-1} + \eta B_H(t) \quad (A2)$$

for the overdamped confined FLE, and

$$x(t) = x_0 - \lambda \int_0^t x(\tau) d\tau + B_H(t) \quad (A3)$$

for confined FBM. These integrals are interpreted trajectorywise, in analogy to Refs. [33,34,36]. We then rescale these equations according to $y \rightarrow y/\sqrt{k_B\mathcal{T}/m\gamma^{1/(2H)}}$ (free FLE motion), $y \rightarrow y/\sqrt{k_B\mathcal{T}/\lambda}$ (confined FLE motion), and $x \rightarrow x/\sqrt{D_H/\lambda^{2H}}$ (confined FBM). The time is rescaled through $t \rightarrow t/\tau$, where τ is the intrinsic time scale of each process. Fractional Brownian motion is rescaled by $B_H \rightarrow (\tau)^{-H} B_H$. Dividing the interval $[0, t]$ into $n + 1$ intervals of even length h , we linearize the fractional derivatives using the results from Diethelm *et al.* [48]

$$\int_0^{t_{n+1}} (t_{n+1} - \tau)^{\alpha-1} f(\tau) d\tau \approx \frac{h^\alpha}{\alpha(\alpha+1)} \sum_{j=0}^{n+1} a_{j,n+1} f(t_j), \quad (\text{A4})$$

where

$$a_{j,n+1} = \begin{cases} n^{\alpha+1} - (n-\alpha)(n+1)^\alpha, & j=0 \\ (n-j+2)^{\alpha+1} + (n-j)^{\alpha+1} - 2(n-j+1)^{\alpha+1}, & 1 \leq j \leq n \\ 1, & j=n+1. \end{cases} \quad (\text{A5})$$

One can then solve for the $v(t_{n+1})$, $y(t_{n+1})$, and $x(t_{n+1})$. This leads in the case of the free FLE to

$$v(t_{n+1}) = \frac{\Gamma(2H+2)}{C} v_0 - \frac{h^{2H}}{C} \sum_{j=0}^n a_{j,n+1} v(t_j) + \frac{\Gamma(2H+2)}{C\sqrt{\Gamma(2H+1)D_H}} B_H(t_{n+1}), \quad (\text{A6})$$

with $C = \Gamma(2H+2) + h^{2H}$ and

$$a_{j,n+1} = \begin{cases} n^{2H+1} - (n-2H)(n+1)^{2H}, & j=0 \\ (n-j+2)^{2H+1} + (n-j)^{2H+1} - 2(n-j+1)^{2H+1}, & 1 \leq j \leq n \\ 1 & j=n+1. \end{cases} \quad (\text{A7})$$

The velocities obtained by this scheme can then be integrated by the trapezoidal rule to obtain the particle position. For the overdamped FLE λ we get

$$y(t_{n+1}) = - \sum_{j=0}^n d_{n+1,j} y(t_j) + \frac{2y_0}{\frac{1}{H} + \Gamma(2H)h^{2-2H}} (n+1)^{2H-1} + \frac{2}{\sqrt{D_H}\Gamma(2H+1)(h + \frac{2h^{2H-1}}{\Gamma(2H+1)})} B_H(t_{n+1}), \quad (\text{A8})$$

with

$$d_{n+1,j} = \begin{cases} \frac{1}{1 + \frac{2h^{2H-2}}{\Gamma(2H+1)}} + \frac{2}{2 + \Gamma(2H+1)h^{2-2H}} [n^{2H} - (n+1-2H)(n+1)^{2H-1}], & j=0 \\ \frac{2}{1 + \frac{2h^{2H-2}}{\Gamma(2H+1)}} + \frac{2}{2 + \Gamma(2H+1)h^{2-2H}} [(n-j+2)^{2H} + (n-j)^{2H} - 2(n-j+1)^{2H}], & 1 \leq j \leq n, \end{cases} \quad (\text{A9})$$

and finally in the case of confined FBM one obtains

$$x(t_{n+1}) = \frac{2-h}{2+h} x(t_n) + \frac{2}{(2+h)\sqrt{D_H}} [B_H(t_{n+1}) - B_H(t_n)]. \quad (\text{A10})$$

Hence we derived expressions for the particle positions or velocities at the time point t_{n+1} depending on all prior positions or velocities. These expressions can be used to obtain trajectories of the corresponding stochastic processes. To simulate FBM, the implementation provided in Refs. [49,50] was used. It is based on a method originally developed by Hosking [51]. It should be noted that all the proposed algorithms have time complexity of order n^2 .

APPENDIX B: SOLUTIONS TO THE STOCHASTIC DIFFERENTIAL EQUATIONS

To analytically solve Eqs. (3), (6), and (8) we formally derive their solutions in Laplace space, treating the noise as a well-behaved function of time, analogously to Deng and Barkai [20]. Averaging and considering that $\langle \xi(s) \rangle = 0$ holds for the Laplace transform of fractional Gaussian noise (2) allows us to identify the first moments (15), (34), (35), and (54). We then multiply each formal solution at two different points in Laplace space. The average of these products gives us the double Laplace transform of the second moments. To obtain explicit expressions, we use the double Laplace transform of fractional Gaussian noise (τ and s being the Laplace variables)

$$\langle \xi(s)\xi(\tau) \rangle = D_H \Gamma(2H+1) \frac{s^{1-2H} + \tau^{1-2H}}{s + \tau}. \quad (\text{B1})$$

The second moments follow as

$$\begin{aligned} \langle y(t_1)y(t_2) \rangle &= \frac{k_B\mathcal{T}}{m} \{ t_1^2 E_{2H,3}(-\gamma t_1^{2H}) + t_2^2 E_{2H,3}(-\gamma t_2^{2H}) - (t_1 - t_2)^2 E_{2H,3}(-\gamma|t_1 - t_2|^{2H}) \} \\ &\quad + \left(v_0^2 - \frac{k_B\mathcal{T}}{m} \right) t_1 t_2 E_{2H,2}(-\gamma t_1^{2H}) E_{2H,2}(-\gamma t_2^{2H}) \end{aligned} \quad (\text{B2a})$$

for free FLE motion,

$$\langle y(t_1)y(t_2) \rangle = \frac{k_B T}{\lambda} A(|t_2 - t_1|) + \left(y_0^2 - \frac{k_B T}{\lambda} \right) A(t_1)A(t_2) + \left(v_0^2 - \frac{k_B T}{m} \right) B(t_1)B(t_2) + y_0 v_0 [A(t_1)B(t_2) + A(t_2)B(t_1)] \quad (\text{B2b})$$

for confined FLE motion [compare Eqs. (30)],

$$\langle y(t_1)y(t_2) \rangle = \frac{k_B T}{\lambda} E_{2-2H} \left(-\frac{\lambda}{\gamma} |t_2 - t_1|^{2-2H} \right) + \left(y_0^2 - \frac{k_B T}{\lambda} \right) E_{2-2H} \left(-\frac{\lambda}{\gamma} t_1^{2-2H} \right) E_{2-2H} \left(-\frac{\lambda}{\gamma} t_2^{2-2H} \right) \quad (\text{B2c})$$

for overdamped confined FLE motion (note that the definitions of γ differ for confined and free FLE motion), and

$$\begin{aligned} \langle x(t_1)x(t_2) \rangle &= D_H \left\{ e^{-\lambda t_1} t_2^{2H} + e^{-\lambda t_2} t_1^{2H} - |t_1 - t_2|^{2H} \right\} + \frac{D_H}{2\lambda^{2H}} \left\{ e^{-\lambda|t_2-t_1|} \gamma(2H+1, \lambda t_1) + e^{\lambda|t_2-t_1|} \gamma(2H+1, \lambda t_2) \right\} \\ &\quad - \frac{D_H}{2\lambda^{2H}} e^{\lambda|t_2-t_1|} \gamma(2H+1, \lambda|t_2-t_1|) - \frac{\lambda D_H}{2(2H+1)} e^{-\lambda(t_2+t_1)} t_1^{2H+1} M(2H+1; 2H+2; \lambda t_1) \\ &\quad - \frac{\lambda D_H}{2(2H+1)} e^{-\lambda(t_2+t_1)} t_2^{2H+1} M(2H+1; 2H+2; \lambda t_2) \\ &\quad + \frac{\lambda D_H}{2(2H+1)} |t_2 - t_1|^{2H+1} e^{-\lambda|t_2-t_1|} M(2H+1; 2H+2; \lambda|t_2-t_1|) + x_0^2 e^{-\lambda(t_1+t_2)} \quad (t_2 > t_1) \end{aligned} \quad (\text{B2d})$$

for confined FBM.

Taken together, the first moments (15), (34), (35), and (54) and the second moments (B2a)–(B2d) compose the full solutions of the stochastic differential equations (3), (6), and (8) [52]. These solutions provide fundamental insight into the behavior of the underlying processes. They allow one to interpret the short- and long-time correlations, capture the complete dynamics of the equilibration, and provide the basis to calculate other valuable quantities such as velocity correlations or the time-averaged MSDs.

APPENDIX C: TIME-AVERAGED MSD FOR CONFINED FBM

For confined FBM the time-averaged MSD takes on the complex form

$$\begin{aligned} \overline{\langle \delta^2(\Delta) \rangle} &= 2D_H \Delta^{2H} + \frac{D_H}{\lambda^{2H}} e^{\lambda \Delta} \gamma(2H+1, \lambda \Delta) - \frac{D_H \lambda}{2H+1} \Delta^{2H+1} e^{-\lambda \Delta} M(2H+1; 2H+2; \lambda \Delta) \\ &\quad + \frac{x_0^2}{2\lambda(T-\Delta)} e^{-2\lambda t_a} (1 - e^{-2\lambda(T-\Delta)}) \{1 + e^{-\lambda \Delta} (e^{-\lambda \Delta} - 2)\} \\ &\quad + (1 - e^{-\lambda \Delta}) \frac{D_H}{(T-\Delta)} \{ (t_a + T - \Delta)^{2H+1} e^{-\lambda(t_a+T-\Delta)} - t_a^{2H+1} e^{-\lambda t_a} \} \\ &\quad + (1 - e^{\lambda \Delta}) \frac{D_H}{(T-\Delta)} \{ (t_a + T)^{2H+1} e^{-\lambda(t_a+T)} - (t_a + \Delta)^{2H+1} e^{-\lambda(t_a+\Delta)} \} \\ &\quad + (1 - e^{-\lambda \Delta}) \frac{D_H}{2(2H+1)(T-\Delta)} \{ (t_a + T - \Delta)^{2H+1} e^{-2\lambda(t_a+T-\Delta)} M(2H+1; 2H+2, \lambda(t_a + T - \Delta)) \\ &\quad - t_a^{2H+1} e^{-2\lambda t_a} M(2H+1; 2H+2, \lambda t_a) \} \\ &\quad + (1 - e^{\lambda \Delta}) \frac{D_H}{2(2H+1)(T-\Delta)} \{ (t_a + T)^{2H+1} e^{-2\lambda(t_a+T)} M(2H+1; 2H+2, \lambda(t_a + T)) \\ &\quad - (t_a + \Delta)^{2H+1} e^{-2\lambda(t_a+\Delta)} M(2H+1; 2H+2, \lambda(t_a + \Delta)) \} \\ &\quad + (1 - e^{-\lambda \Delta}) \frac{D_H}{\lambda^{2H}(T-\Delta)} \left\{ \gamma(2H+1, \lambda(t_a + T - \Delta)) \left(t_a + T - \Delta - \frac{4H-1}{2\lambda} \right) - \gamma(2H+1, \lambda t_a) \left(t_a - \frac{4H-1}{2\lambda} \right) \right\} \\ &\quad + (1 - e^{\lambda \Delta}) \frac{D_H}{\lambda^{2H}(T-\Delta)} \left\{ \gamma(2H+1, \lambda(t_a + T)) \left(t_a + T - \frac{4H-1}{2\lambda} \right) - \gamma(2H+1, \lambda(t_a + \Delta)) \left(t_a + \Delta - \frac{4H-1}{2\lambda} \right) \right\}. \end{aligned} \quad (\text{C1})$$

- [1] E. Barkai, Y. Garini, and R. Metzler, *Phys. Today* **65**(8), 29 (2012).
 [2] I. M. Sokolov, *Soft Matter* **8**, 9043 (2012).
 [3] J. H. P. Schulz, E. Barkai, and R. Metzler, *Phys. Rev. Lett.* **110**, 020602 (2013).
 [4] Y. He, S. Burov, R. Metzler, and E. Barkai, *Phys. Rev. Lett.* **101**, 058101 (2008).

- [5] S. Burov, J.-H. Jeon, R. Metzler, and E. Barkai, *Phys. Chem. Chem. Phys.* **13**, 1800 (2011).
 [6] E. W. Montroll and G. H. Weiss, *J. Math. Phys.* **6**, 167 (1965); H. Scher and E. W. Montroll, *Phys. Rev. B* **12**, 2455 (1975).
 [7] J.-P. Bouchaud, *J. Phys. I (Paris)* **2**, 1705 (1992); G. Bel and E. Barkai, *Phys. Rev. Lett.* **94**, 240602 (2005); A. Rebenshtok and E. Barkai, *ibid.* **99**, 210601 (2007).

- [8] A. Lubelski, I. M. Sokolov, and J. Klafter, *Phys. Rev. Lett.* **100**, 250602 (2008).
- [9] This is defined in terms of the stationary distribution $P_{st}(x) = \lim_{t \rightarrow \infty} P(x, t)$ as $\langle x^2 \rangle_{th} = \int x^2 P_{st}(x) dx$.
- [10] S. Burov, R. Metzler, and E. Barkai, *Proc. Natl. Acad. Sci. U.S.A.* **107**, 13228 (2010).
- [11] T. Neusius, I. M. Sokolov, and J. C. Smith, *Phys. Rev. E* **80**, 011109 (2009).
- [12] J.-H. Jeon, V. Tejedor, S. Burov, E. Barkai, C. Selhuber-Unkel, K. Berg-Sørensen, L. Oddershede, and R. Metzler, *Phys. Rev. Lett.* **106**, 048103 (2011).
- [13] A. V. Weigel, B. Simon, M. M. Tamkun, and D. Krapf, *Proc. Natl. Acad. Sci. U.S.A.* **108**, 6438 (2011).
- [14] S. M. A. Tabei, S. Burov, H. Y. Kim, A. Kuznetsov, T. Huynh, J. Jureller, L. H. Philipson, A. R. Dinner, and N. F. Scherer, *Proc. Natl. Acad. Sci. U.S.A.* **110**, 4911 (2013).
- [15] M. Magdziarz, R. Metzler, W. Szczotka, and P. Zebrowski, *Phys. Rev. E* **85**, 051103 (2012); V. Tejedor and R. Metzler, *J. Phys. A* **43**, 082002 (2010).
- [16] M. A. Lomholt, L. Lizana, R. Metzler, and T. Ambjörnsson, *Phys. Rev. Lett.* **110**, 208301 (2013).
- [17] A. G. Cherstvy, A. V. Chechkin, and R. Metzler, *New J. Phys.* **15**, 083039 (2013); A. G. Cherstvy and R. Metzler, *Phys. Chem. Chem. Phys.* **15**, 20220 (2013).
- [18] G. Zumofen and J. Klafter, *Physica D* **69**, 436 (1993); D. Froemberg and E. Barkai, *Phys. Rev. E* **87**, 030104(R) (2013); A. Godec and R. Metzler, *Phys. Rev. Lett.* **110**, 020603 (2013).
- [19] E. Barkai and Y.-C. Cheng, *J. Chem. Phys.* **118**, 6167 (2003); E. Barkai, *Phys. Rev. Lett.* **90**, 104101 (2003).
- [20] W. Deng and E. Barkai, *Phys. Rev. E* **79**, 011112 (2009).
- [21] J.-H. Jeon and R. Metzler, *Phys. Rev. E* **81**, 021103 (2010).
- [22] J.-H. Jeon and R. Metzler, *Phys. Rev. E* **85**, 021147 (2012).
- [23] The additional factor of 2 arises from the definition of the time-averaged MSD; compare Eq. (18).
- [24] F. Höfling and T. Franosch, *Rep. Prog. Phys.* **76**, 046602 (2013).
- [25] I. Goychuk, *Phys. Rev. E* **80**, 046125 (2009); *Adv. Chem. Phys.* **150**, 187 (2012).
- [26] J. Szymanski and M. Weiss, *Phys. Rev. Lett.* **103**, 038102 (2009).
- [27] L. P. Sanders and T. Ambjörnsson, *J. Chem. Phys.* **136**, 175103 (2012); L. Lizana, T. Ambjörnsson, A. Taloni, E. Barkai, and M. A. Lomholt, *Phys. Rev. E* **81**, 051118 (2010).
- [28] I. Bronstein, Y. Israel, E. Kepten, S. Mai, Y. Shav-Tal, E. Barkai, and Y. Garini, *Phys. Rev. Lett.* **103**, 018102 (2009); K. Burnecki, E. Kepten, J. Janczura, I. Bronshtein, Y. Garini, and A. Weron, *Biophys. J.* **103**, 1839 (2012).
- [29] S. C. Weber, A. J. Spakowitz, and J. A. Theriot, *Phys. Rev. Lett.* **104**, 238102 (2010).
- [30] J.-H. Jeon, H. Martinez-Seara Monne, M. Javanainen, and R. Metzler, *Phys. Rev. Lett.* **109**, 188103 (2012); G. R. Kneller, K. Baczyński, and M. Pasenkiewicz-Gierula, *J. Chem. Phys.* **135**, 141105 (2011).
- [31] J.-H. Jeon, N. Leijnse, L. Oddershede, and R. Metzler, *New J. Phys.* **15**, 045011 (2013).
- [32] R. Kubo, *Rep. Prog. Phys.* **29**, 255 (1966).
- [33] B. B. Mandelbrot and J. W. van Ness, *SIAM Rev.* **10**, 422 (1968).
- [34] G. Gripenberg and I. Norros, *J. Appl. Probab.* **33**, 400 (1996).
- [35] E. Lutz, *Phys. Rev. E* **64**, 051106 (2001).
- [36] S. C. Kou, *Ann. Appl. Stat.* **2**, 501 (2008).
- [37] W. Min, G. Luo, B. J. Cherayil, S. C. Kou, and X. S. Xie, *Phys. Rev. Lett.* **94**, 198302 (2005).
- [38] R. Kupferman, *J. Stat. Phys.* **114**, 291 (2004).
- [39] A. N. Kolmogorov, *Dokl. Akad. Nauk SSSR* **26**, 115 (1940).
- [40] A. Weron and M. Magdziarz, *Europhys. Lett.* **86**, 60010 (2009).
- [41] N. N. Pottier, *Physica A* **317**, 371 (2003).
- [42] *Higher Transcendental Functions*, edited by H. Bateman and A. Erdélyi, Bateman Manuscript Project Vol. III (McGraw Hill, New York, 1955).
- [43] P. Siegle, I. Goychuk, and P. Hänggi, *Phys. Rev. Lett.* **105**, 100602 (2010).
- [44] P. Siegle, I. Goychuk, P. Talkner, and P. Hänggi, *Phys. Rev. E* **81**, 011136 (2010).
- [45] S. Burov and E. Barkai, *Phys. Rev. Lett.* **100**, 070601 (2008); *Phys. Rev. E* **78**, 031112 (2008).
- [46] M. Abramowitz and I. A. Stegun, *Handbook of Mathematical Functions* (Dover, New York, 1972).
- [47] O. Yu. Sliusarenko, V. Yu. Gonchar, A. V. Chechkin, I. M. Sokolov, and R. Metzler, *Phys. Rev. E* **81**, 041119 (2010).
- [48] K. Diethelm, N. J. Ford, and A. D. Freed, *Nonlinear Dynam.* **29**, 3 (2002).
- [49] A. B. Dieker, M.Sc. thesis, Vrije Universiteit Amsterdam, 2004.
- [50] A. B. Dieker and M. Mandjes, *Probab. Eng. Inf. Sci.* **17**, 417 (2003).
- [51] J. R. M. Hosking, *Water Resour. Res.* **20**, 1898 (1984).
- [52] N. G. Van Kampen, *Stochastic Processes in Physics and Chemistry* (North-Holland, Amsterdam, 2007).